Dynamic Compact Thermal Model of an Electrothermal Micromirror Based on Transmission Line Theory

Sagnik Pal* and Huikai Xie**

Department of Electrical and Computer Engineering, University of Florida, Gainesville, FL 32611
*sagnik@ufl.edu **hkx@ufl.edu

ABSTRACT

A procedure for building a parametric dynamic thermal model of electrothermally-actuated devices is developed and demonstrated using a 1-D scanning micromirror. The micromirror is actuated by thermal bimorphs and an embedded platinum (Pt) resistor is used for generating Joule heating. The thermal model is developed by drawing analogy between heat flow in the device and current-flow through an electrical transmission line. It provides the temperature of the embedded heater and the bimorph actuators. The distributed thermal impedances of the transmission-line model are represented by an equivalent circuit model with a few elements. A simplification of the circuit model is proposed when small length scales are involved. Rotation angle per unit power input predicted by the circuit model has an error of less than 8% compared to experimental results. The low-frequency decay in device response is accurately predicted.

Keywords: dynamic thermal model, compact thermal model, transmission-line, lumped element, micromirror

1 INTRODUCTION

Several electrothermal MEMS devices such as micromirrors [1], tunable inductors [2], track-positioning systems for optical disk drives [3] have been reported in literature. Electrothermal actuation is achieved by using a heating source, such as a resistive heater, to generate thermally induced strain and produce motion.

Comprehensive electrothermomechanical modeling is essential for quantifying the dependence of device response on device parameters, achieving proper thermal management, preventing device damage due to overheating, and meeting device performance requirements. Fig. 1 shows the schematic of an electrothermal micromirror model [4]. The schematic is generic and can be adapted to a wide range of electrothermal MEMS. As shown in Fig. 1, the complete model consists of electrothermal, thermal and mechanical sub-models. The power consumption and response time of most electrothermal MEMS is determined by the thermal model. This paper focuses on developing a dynamic thermal model of an electrothermal micromirror.

Several approaches for thermal modeling are available in literature. Analytical methods are limited to simple geometries only. Numerical techniques such as finite element (FE) and finite difference methods are accurate but they consume significant time and resources. Also, they are not parametric, *i.e.*, they do not provide a direct relationship between device response and device parameters [4].

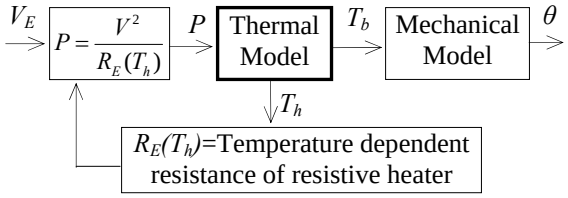

Figure 1: Schematic of a complete model of an electrothermally-actuated micromirror. V_E=applied voltage, P=power dissipated by Joule heating, T_b=average bimorph actuator temperature, θ=mirror rotation angle, T_h=temperature of embedded resistive heater and $R_E(T_h)$=resistance of embedded heater [4].

A thermal model may be represented as an RC network in which resistors, capacitors, current and voltage represent thermal resistances, thermal capacitances, heat flow and temperature respectively [4]. Practical problems may involve a large number of circuit elements making them computationally cumbersome [5]. Székely *et al.* defined a time constant density function for distributed RC networks which may be evaluated using numerical solvers such as SUNRED [6]; dominant time constants may then be chosen to construct lumped element models (LEM) [6]. Christiaens *et al.* reported a compact RC network thermal model for a PSGA package [7]. However, the network topology is chosen by intuition rather than rigorous guidelines.

Computational resource and simulation time requirements can be reduced significantly by extracting reduced order models (ROM) from FE models. Order reduction does not affect computational accuracy significantly. However, ROMs are not parametric. The authors reported a thermal ROM of an electrothermal micromirror from which a heuristic parametric LEM was built [8]. However, rigorous guidelines for building a parametric LEM have not been established. By drawing upon the analogy between electrical transmission line and heat flow, the authors have built a static thermal model of an electrothermal micromirror and established a rigorous approach for simplifying the transmission-line model (TLM) to obtain an LEM [4]. In this paper, a dynamic

thermal model of an electrothermal micromirror based on TLM is developed.

The next section describes an electrothermal micromirror. Section 3 introduces FE model and TLM. Experimental results are provided in Section 4.

2 DEVICE DESCRIPTION

Figs. 2 and 3 show the SEM and schematic of the electrothermal micromirror. The mirror plate is attached to the substrate by an array of 72 thermal bimorph actuators. The difference in thermal expansion coefficient (TEC) of the SiO_2 and Al layers causes the bimorphs to bend, thereby causing the mirror plate to tilt. At either ends of the bimorphs, SiO_2 thermal isolation limits the flow of heat from the bimorphs to the mirror plate and the substrate. Detailed device description is available in [4].

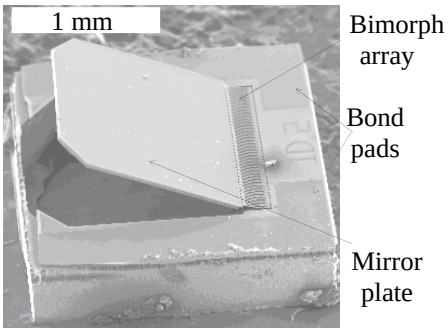

Figure 2: SEM of electrothermal micromirror [4].

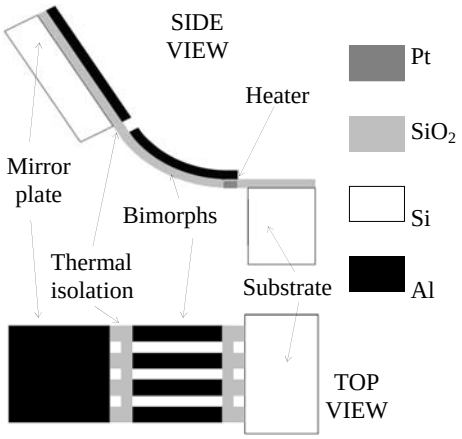

Figure 3: Schematic of electrothermal micromirror [4].

Neglecting end effects at either extremes of the actuator array, the bimorphs have a nearly identical temperature distribution [4]. The mirror tilt angle θ is given by [4],

$$\theta(T_b) = \theta_0 + \lambda \times (T_b - T_0) \quad (1)$$

where T_b is the average temperature along the bimorph length, θ_0 is the mirror-tilt angle when $T_b=T_0$. The constant λ=0.08673 °/K. For an applied voltage, V_E, the power dissipated, P, in the embedded heater is,

$$P = \frac{V_E^2}{R_{E0}(1+\alpha(T_h - T_0))} \quad (2)$$

where T_h is the embedded heater temperature, R_{E0} is the resistance when the heater is at reference temperature T_0. For T_0=298 K, the temperature coefficient of resistance (TCR) α=0.0025 K^{-1} [4].

From (1) and (2), the values of T_b and T_h are of interest to the engineer. The thermal model of the micromirror that takes P as input and evaluates T_b and T_h as outputs will be discussed next.

3 THERMAL MODEL

3.1 Thermal FE model of micromirror

As mentioned in Section 2, most bimorphs have a nearly identical temperature distribution. Fig. 4 shows a thermal FE model of a bimorph and a section of the mirror plate attached to it [4].

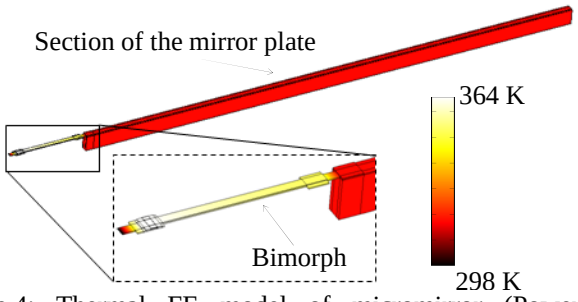

Figure 4: Thermal FE model of micromirror (Power input=10 mW) [4]

From the FE model it is found that temperature gradient occurs mainly along the length of the bimorph and mirror-plate section. Therefore, 1-D heat flow may be assumed. A generic thermal model for 1-D heat flow will be developed in the next section.

3.2 TLM for a 1-D geometry

Let us consider heat flow through a 1-D geometry of uniform cross-section area A and length l that is oriented along the x axis. Let the thermal conductivity be k and the heat capacitance per unit length be c. If the 1-D geometry consists of layers of different materials, the equivalent thermal conductivity is obtained by taking the weighted average of thermal conductivities of all the layers with the weights as the layer thicknesses. The equivalent thermal resistance per unit length is $r=1/(kA)$. Let g represent the thermal conductance per unit length. The thermal conductance accounts for heat loss due to convection and diffusion to the surroundings. A discussion on heat loss coefficient is provided in [4]. The thermal model may be represented by the two-port distributed network shown in Fig. 5(a) [9]. An infinitesimal element is represented by resistors $r\Delta x$ and $1/(g\Delta x)$ and the capacitor $c\Delta x$; and a series of such infinitesimal elements represent thermal impedances in the complete length l of the 1-D geometry. The voltage, v, denotes the increase in temperature above the ambient. The current, i, represents heat flow. Principles

governing transmission lines are well established [10] and may be used to analyze the circuit shown in Fig. 5(a). At *x,* let the voltage be $v(x)$ and the current be $i(x)$.

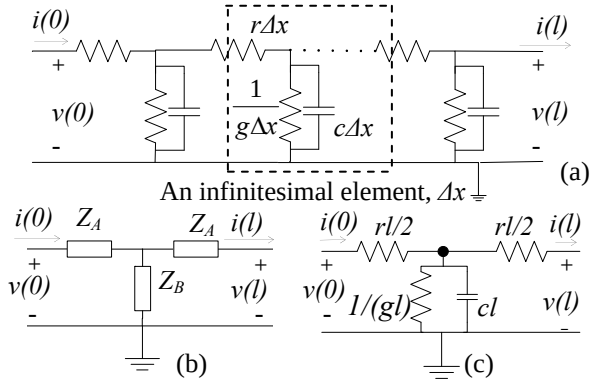

Figure 5: (a) Transmission-line model for 1-D heat flow (b) Equivalent two port network (c) Approximate LEM

Assuming harmonic dependence,

$$v(x,t) = \mathrm{Re}(V(x)e^{j\omega t}) \tag{3}$$

$$i(x,t) = \mathrm{Re}(I(x)e^{j\omega t}) \tag{4}$$

Let,

$$\gamma = \sqrt{r(g + j\omega c)} \tag{5}$$

The well known transmission line equations are [10],

$$V(x) = (A_1 e^{-\gamma x} + A_2 e^{\gamma x}) \tag{6}$$

$$I(x) = \frac{\gamma}{r}(A_1 e^{-\gamma x} - A_2 e^{\gamma x}) \tag{7}$$

The constants A_1 and A_2 can be determined by the heat sources and thermal impedances connected at the two ends of the 1-D geometry. The TLM depicted in Fig. 5(a) may be equivalently represented by the two-port network shown in Fig. 5(b). Comparing the *ABCD* parameters of the networks shown in Figs. 5(a) and 5(b),

$$Z_A = \frac{r}{\gamma}\frac{e^{\gamma l} - 1}{e^{\gamma l} + 1} = Z_0 \times \tanh(\gamma l / 2) \tag{8}$$

$$Z_B = \frac{r}{\gamma}\frac{2e^{\gamma l}}{e^{2\gamma l} - 1} = \frac{Z_0}{\sinh(\gamma l)} \tag{9}$$

where,

$$Z_0 = r / \gamma \tag{10}$$

The circuit model shown in Fig. 5(b) has been rigorously derived and accounts for the distributed nature of thermal resistances. Since MEMS devices involve small length scales, it may be possible to approximate the hyperbolic functions in (8) and (9) by using Taylor series expansion. Expanding (8) and using (5) and (10),

$$Z_A = Z_0(\gamma l/2 - \frac{(\gamma l/2)^3}{3} + \frac{2(\gamma l/2)^5}{15}\cdots) \approx \frac{Z_0 \gamma l}{2} = \frac{rl}{2} \tag{11}$$

Expanding (9) and using (5) and (10),

$$Z_B = \frac{Z_0}{\gamma l + \frac{(\gamma l)^3}{6} + \frac{(\gamma l)^5}{120}\cdots} \approx \frac{Z_0}{\gamma l} = \frac{1}{(gl + j\omega cl)} \tag{12}$$

The approximations used in (11) and (12) are valid if,

$$\left|\mathrm{Re}(\gamma l)^3\right| \ll \left|\mathrm{Re}(\gamma l)\right| \tag{13}$$

$$\left|\mathrm{Im}(\gamma l)^3\right| \ll \left|\mathrm{Im}(\gamma l)\right| \tag{14}$$

Equations (11) and (12) have been used to build the thermal LEM shown in Fig. 5(c). Fig. 5(c) elucidates the physical significance of Z_A and Z_B. From (11), $Z_A \approx rl/2$ represents half of the conductive resistance of the 1-D geometry. Similarly, from (12), Z_B represents the parallel connection of a resistor ($1/(gl)$) and a capacitor cl. Hence, the heat loss to the atmosphere and the total capacitance are lumped together as Z_B.

Substituting (5) and simplifying (13) and (14) gives,

$$(rl)(gl) \ll 1 \Rightarrow l << 1/\sqrt{rg} \tag{15}$$

$$(rl)(cl) \ll 1/\omega \Rightarrow l << 1/\sqrt{\omega rc} \tag{16}$$

We conclude that if (15) and (16) are satisfied, the LEM shown in Fig. 5(c) can be used without incurring a large error. Otherwise the 1-D geometry may be partitioned into smaller segments such that (15) and (16) are satisfied by each segment.

These results will be applied to develop a thermal model of the micromirror in the next subsection.

3.3 TLM for electrothermal micromirror

Fig. 6 shows the thermal model of the micromirror. The subscripts *b* and *m* represent the bimorph and the mirror respectively. The number of bimorphs is *n*. Since the thermal isolation regions are more than an order of magnitude smaller than the bimorphs, their thermal capacitance and conductance are neglected. R_{iso1} and R_{iso2} represent the conductive thermal resistances of the isolation regions.

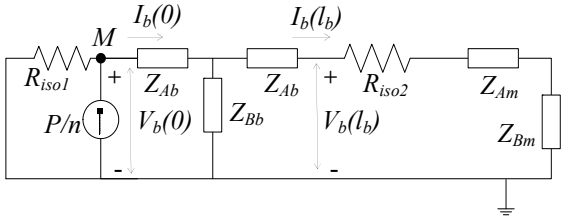

Figure 6: Thermal model of micromirror based on rigorous transmission-line theory

The average bimorph temperature rise, ΔT_b, may be obtained by integrating (6) over l_b.

$$\Delta T_b = \mathrm{Re}[\frac{\int_0^{l_b} V_b(x)dx}{l_b} e^{j\omega t}] = \mathrm{Re}[\frac{(1 - e^{-\gamma_b l_b})(A_{1b} + A_{2b}e^{\gamma_b l_b})}{l_b \gamma_b} e^{j\omega t}] \tag{17}$$

The voltage at node *M* gives the rise in heater temperature,

$$\Delta T_h = \mathrm{Re}[V(0)e^{j\omega t}] = \mathrm{Re}[(A_{1b} + A_{2b})e^{j\omega t}] \tag{18}$$

Let, $Z_L = R_{iso1}$ and $Z_R = R_{iso2} + Z_{Am} + Z_{Bm}$ denote the impedances to the left and right of the bimorph. Equating the impedances Z_L and Z_R to the ratio of voltage and current at either extreme of the bimorph,

$$A_{1b} = \frac{e^{2l_b\gamma_b}(P/n)r_b Z_L(r_b + Z_R\gamma_b)}{-(r_b - Z_L\gamma_b)(r_b - Z_R\gamma_b) + e^{2l_b\gamma_b}(r_b + Z_L\gamma_b)(r_b + Z_R\gamma_b)} \tag{19}$$

$$A_{2b} = \frac{-(P/n)r_b Z_L (r_b - Z_R\gamma_b)}{-(r_b - Z_L\gamma_b)(r_b - Z_R\gamma_b) + e^{2l_b\gamma_b}(r_b + Z_L\gamma_b)(r_b + Z_R\gamma_b)} \quad (20)$$

It was experimentally found that for frequencies greater than f_{limit}=265 Hz, *i.e.*, ω_{limit}=1665 rad/s, the mirror deflection is negligible. Therefore, it is desirable to have a thermal model that is accurate in the 0–265 Hz frequency range. In accordance with (15) and (16) the bimorph was partitioned into 8 segments. Fig. 7 shows the electrothermal LEM. Since the mirror-plate is an order of magnitude thicker than the bimorphs, its conductive thermal resistance is neglected. The average bimorph temperature is obtained from the ammeter output,

$$\Delta T_b = \frac{1}{8}\sum_{i=1}^{8} V_i = \frac{1}{8}\left(\frac{8}{g_b l_b}\right)\sum_{i}^{8} I_i = \frac{I_{total}}{g_b l_b} \quad (21)$$

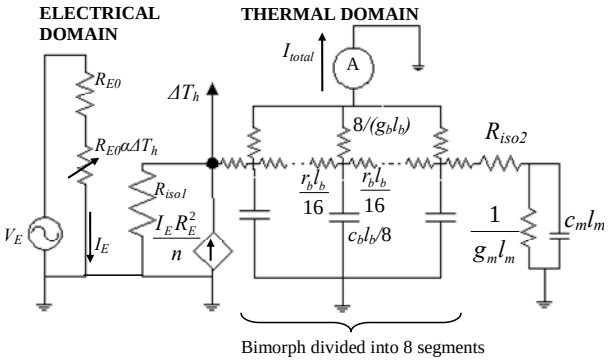

Figure 7: Electrothermal LEM of the micromirror

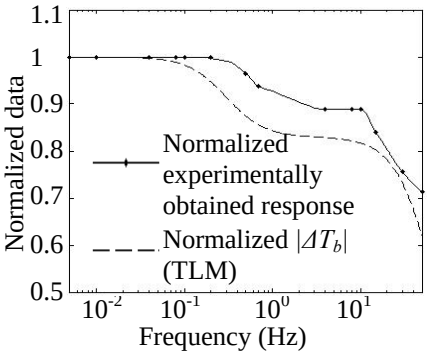

Figure 8: Comparison of TLM with dynamic experimental data obtained by monitoring a laser beam reflected from the scanning mirror

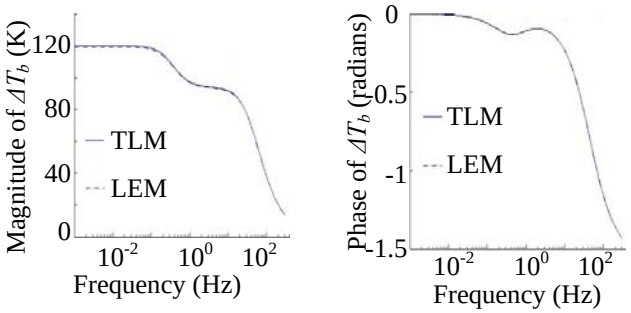

Figure 9: Comparison between TLM and LEM up to 300 Hz (a) Magnitude response (b) Phase response

4 RESULTS

Mirror deflections predicted by static TLM and LEM are in good agreement with experimental results to within 8% [4]. Fig. 8 compares the experimentally obtained frequency response with TLM output. Clearly, TLM accurately predicts the range of frequencies over which the response decays. Fig. 9 compares TLM and LEM outputs. Good agreement is observed up to 300 Hz.

5 SUMMARY AND DISCUSSION

We report a general procedure for building a dynamic model of electrothermal devices and demonstrate it with a micromirror device. The thermal model may be integrated with the electrothermal and mechanical models to generate the complete device model. A thermal FE model is built. A circuit model that predicts the thermal behavior is then developed by drawing analogy between heat transfer and transmission lines. A simplification of the circuit model into an LEM is proposed when small length scales are involved. The FE, circuit and lumped element models show good agreement with experimental results. The model developed in this paper is parametric, *i.e.*, the device parameters can be varied. Therefore, it is useful for design and optimization. Future work will involve the development of a comprehensive parametric dynamic electro-thermo-mechanical model. This project is supported by the National Science Foundation under award# 0901711.

REFERENCES

[1] G. Lammel et al., "Optical Microscanners and Microspectrometers using Thermal Bimorph Actuators," Boston: Kluwer Academic Pub., 2002

[2] I. Zine-El-Abidine, M. Okoniewski, and J. G. McRory, J. Micromech. Microeng., 15, 2063, 2005.

[3] J. P. Yang, X. C. Deng, and T. C. Chong,, J. Micromech. Microeng., 15, 958, 2005.

[4] S. Pal and H. Xie, J. Micromech. Microeng., 20, 045020, 2010.

[5] X. Gui, P. W. Webb, and G. B. Gao, IEEE Trans. on Electron Devices, 39, 1295–1302, 1992.

[6] V. Székely, A. Páhi, M. Rosental, and M. Rencz, Proc. of MSM, Puerto Rico, 342–345, 1999.

[7] F. Christiaens, B. Vandevelde, E. Beyne, R. Mertens, and J. Berghmans, IEEE Trans. on Components, Packaging, and Manufacturing Technology, Part A, 21, 565–576, 1998.

[8] S. Pal and H. Xie, J. Micromech. Microeng., 19, 065007, 2009.

[9] V. Székely and M. Rencz, IEEE Trans. on components and packaging, 23(3), 587–594, 2000.

[10] M. N. O. Sadiku, "Elements of electromagnetics," New York: Saunders College Pub., 1989.